

## Optimization study on roof break direction of gob-side entry retaining by roof break and filling in thick-layer soft rock layer

Dang-Wei Yang<sup>1,2a</sup>, Zhan-Guo Ma<sup>\*1,2</sup>, Fu-Zhou Qi<sup>1,2</sup>, Peng Gong<sup>1,2</sup>,  
Dao-Ping Liu<sup>1,2</sup>, Guo-Zhen Zhao<sup>3</sup> and Ray Ruichong Zhang<sup>4</sup>

<sup>1</sup> State Key Laboratory for Geomechanics & Deep Underground Engineering,  
China University of Mining and Technology, Xuzhou, China

<sup>2</sup> School of Mechanics & Civil Engineering, China University of Mining and Technology, Xuzhou, China

<sup>3</sup> College of Mining Engineering, Taiyuan University of Technology, Taiyuan, China

<sup>4</sup> Division of Engineering, Colorado School of Mines, Golden, CO, USA

(Received November 18, 2016, Revised February 22, 2017, Accepted March 03, 2017)

**Abstract.** This paper proposes gob-side entry retaining by roof break and filling in thick-layer soft rock conditions based on the thick-layer soft rock roof strata migration law and the demand for non-pillar gob-side entry retaining projects. The functional expressions of main roof subsidence are derived for three break roof direction conditions: lateral deflection toward the roadway, lateral deflection toward the gob and vertically to the roof. These are derived according to the load-bearing boundary conditions of the main roadway roof stratum. It is concluded that the break roof angle is an important factor influencing the stability of gob-side entry retaining surrounding rock. This paper studies the stress distribution characteristics and plastic damage scope of gob-side entry retaining integrated coal seams, as well as the roof strata migration law and the supporting stability of caving structure filled on the break roof layer at the break roof angles of  $-5^\circ$ ,  $0^\circ$ ,  $5^\circ$ ,  $10^\circ$  and  $15^\circ$  are studied. The simulation results of numerical analysis indicate that, the stress concentration and plastic damage scope to the sides of gob-side entry retaining integrated coal at the break roof angle of  $5^\circ$  are reduced and shearing stress concentration of the caving filling body has been eliminated. The disturbance of coal mining to the roadway roof and loss of carrying capacity are mitigated. Field tests have been carried out on air-return roadway 5203 with the break roof angle of  $5^\circ$ . The monitoring indicates that the break roof filling section and compaction section are located at 0-45 m and 45-75 m behind the working face, respectively. The section from 75-100 m tends to be stable.

**Keywords:** thick-layer soft rock; break roof filling; gob-side entry retaining; filling support structure; break roof angle

### 1. Introduction

In recent years, the development of coal mining has tended towards increasing efficiency and economization. As one important technology in scientific and efficient mining, non-pillar gob-side entry retaining technology has been widely applied in long-wall mining systems. Non-pillar gob-side entry retaining technology refers to re-supporting the previous Sectional Horizontal Roadway

---

\*Corresponding author, Professor, E-mail: addresses: [zgma@cumt.edu.cn](mailto:zgma@cumt.edu.cn)

<sup>a</sup> E-mail: [lansebingling2016@163.com](mailto:lansebingling2016@163.com)

along the gob side edge at the rear of the mining working face with certain technological means, so as to allow its continuous service at the next Sectional Horizontal Roadway. In comparison with the traditional long-wall mining system which includes some roadway protection methods to protect the coal pillar non-pillar gob-side entry retaining technology not only cancels the protective coal pillar to improve the resources recovery rate, reduce tunneling and maintenance costs of roadways, but also avoids disasters such as rock bursts and gas outbursts caused by protective coal pillars (Wang *et al.* 2015 and Ning *et al.* 2014). Furthermore, it reduces the discarded gangue accumulated on the ground and alleviates the environmental pollution. Accordingly, economic and social benefits have been achieved in mine production.

To implement gob-side entry retaining, it is important to consider the impact of the structural evolution process of the overlying strata and stress distribution laws on rock deformation on the surrounding retaining roadway. Packaged gob-side entry retaining technology with roadside and roadin pack structures as the core has been formed gradually on the basis of research and practice by scholars and site technicians at home and abroad and has been widely applied. Such technology is complicated and has high requirements for site construction management. Its adaptability to coal seam geological occurrence conditions is low and its construction cost is high, restricting its application and development. The research in recent years indicates that the large-area hanging roof at the rear of the gob is the main factor affecting the stability of gob-side entry retaining. The implementation of break roof technology to the lateral roof of the roadway changes the structure of special rock masses by means of manual intervention. As a result, not only is the stress distribution is optimized, but also adverse factors, such as plastic damage and crack extension, are controlled. Based on the principle above, it is proposed to implement roof cut and pressure releasing gob-side entry retaining technology is proposed to be implemented in thin coal seams with solid roofs (Zhang *et al.* 2011), to conduct advance presplitting on the gob-side roadway to cut the connection of the gob-side roadway roof and immediate and main stope roof. Under the pressure effect of the mine, the stope roof cracks along the presplitting face. Such technology not only does away with the roadside and in-road filling wall to simplify the entry retaining and reduce the supporting costs, but also cuts the connection of the gob and overlying rock of the roadway, to transfer the stress concentration of roadway surrounding rock and improve its stress environment. Such technology is applicable to thin coal seams with solid roofs. Consequently, breaking a key pressure-bearing key layer in the roof of the roadway, the overlying rock migrates nonviolently and is not easily led to separation, and the roadway is easy to maintain. The collapsed rock is only used as a wall to block and isolate the gob side (Tan *et al.* 2015). Medium-thickness coal seams with thick soft roofs are distributed widely in China. The coal seam roof strata have loose and broken mechanical properties and low strength, so the fracture development easily causes collapse (Nguyen *et al.* 2011). In addition, there is no evident key pressure-bearing layer, and the overlying rock migrates in a complex fashion. Consequently, it is difficult to control the roadway surroundings and apply gob-side entry retaining technology (Taheri and Tani 2010 and Zhu *et al.* 2013). This paper sets forth a technology to fill the gob-side entry retaining on the thick-layer soft roof break roof layer with respect to the geological occurrence features of coal seam 5# with a thick-layer soft roof in Changxing coal mine, China. With this technology, the collapsed rock filling the roadway gob side, not only forms a gangue wall, but also employs the bulking characteristics of the collapsed rock to come into contact with the overlying stable rock, and guarantee the stability of the soft rock roadway surrounding rock.

## 2. Proposal of technology to fill gob-side entry retaining on break roof layer

### 2.1 Geological occurrence conditions

The coal seam 5# at a mine has an average thickness of 2 m, belonging to medium-thickness coal seams. As shown in the geology columnar Fig. 1, the immediate roof stratum of the coal seam is black mudstone with the average thickness of 3.3 m, weak carrying capacity, and crushing, abscission layer are liable to occur. The main roof stratum is sandy mudstone with the average thickness of 3.1 m, good stability, having direct impact on the roadway pressure (Fan *et al.* 2010). The main roof stratum has sandy mudstone with the average thickness of 7.7 m at the top. The overlying rock of coal seam 5# is the thick-layer soft compound rock strata, mainly mudstone strata and sandy mudstone strata. It has low strength and weak carrying capacity. Under the effect of mining disturbance, fracture development and rock mass breaking may occur, so it is hard to maintain (Li and Li 2016).

### 2.2 Strata structure analysis for filling gob-side entry retaining on break roof layer

The rotary subsidence of the overlying rift block at the gob side will lead to continuous pressurization (Zhao 2015). The longer the rotary subsidence lasts, the longer the disturbance to the roadway lasts (Li *et al.* 2016a). Filling of gob-side entry retaining on the thick-layer soft break roof layer implements roof breaking on the gob side of the thick-layer soft rock roof to cut the connection of the roadway main roof and overlying rock at the gob side, It also shortens the hanging length of the roof rock beam at the roadway gob, expedites the roof breaking and subsidence at the gob, weakens the overlying rock pressure caused by mining at the working face and significantly shortens the movement time of the roof and disturbance period of entry retaining. Meanwhile, under the effect of its own gravity, overlying rock pressure and mining disturbance, the soft rock strata will be broken and shattered. By using the bulking characteristics of the collapsed rock, the roadside gob is filled to form the first retained roadway of the gangue wall and

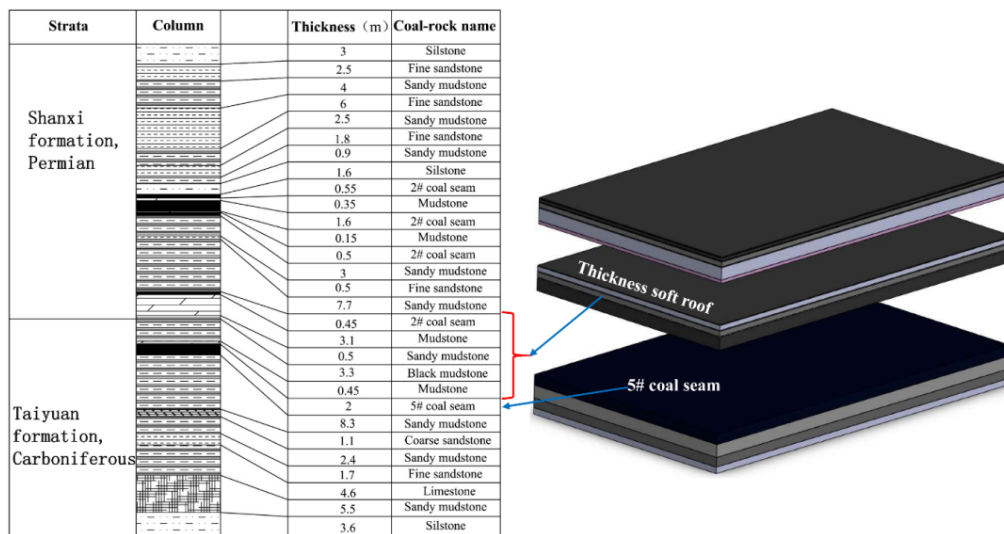
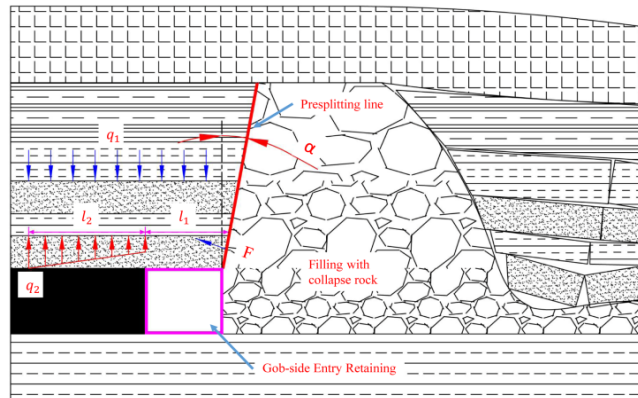
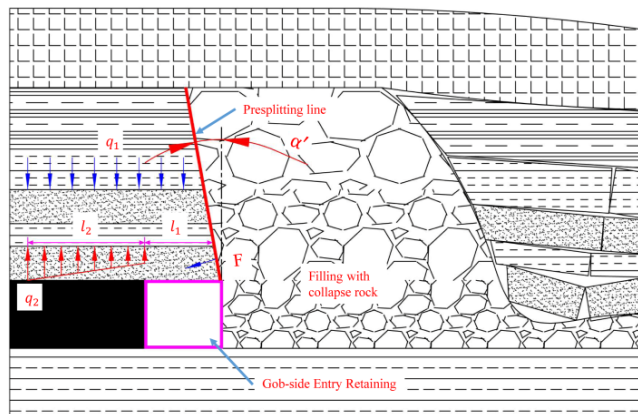


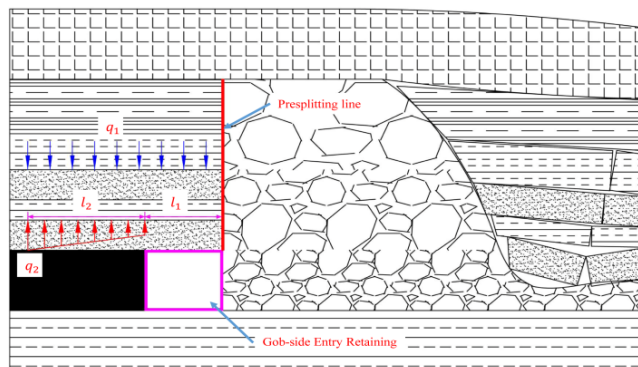
Fig. 1 Generalized stratigraphic column



(a) Deflection toward the gob overlying strata structure



(b) Deflection toward the roadway overlying strata structure



(c) Vertically to the roof overlying strata structure

Fig. 2 Overlying strata structure of gob-side entry retaining

make contact with the overlying stable rock. Through compaction, the bearing structure is formed at the area of gob-side entry retaining to support overlying rock pressure and form the coordinated control structure of the roadway surrounding rock by “roof breaking and pressure releasing + filling with collapsed rock”.

As the working face advances, the hanging area of the roadway main roof will increase. The main roof will be bent and sink along the interface of the break roof layer and be compacted in contact with the caving filling structure of the break roof layer. At this moment, the main roof can be deemed a cantilever structure. The presplitting break roof layer angle can be divided into three roof breaking methods: deflection to the gob side of roadway, deflection to the roadway side deflection and vertically to the roadway roof. Different break roof layer directions and inclinations will change the boundary stress conditions of gob-side entry retaining and the subsidence functional expression  $\omega$  of the roadway main roof obtained according to the boundary conditions. Fig. 2(a) deflection to the gob side of roadway, when  $0 < x < l_2$ ,

$$\begin{aligned} \omega_1 = & \frac{q_1 x^2}{24EI} [x^2 + 6(l_1 + l_2)^2 - 4(l_1 + l_2)x] - \frac{q_2 x^2}{120EI l_2} (10l_2^3 - 10l_2^2 x + 5l_2 x^2 - x^3) \\ & + \frac{F \sin \alpha x^2}{6EI} [3(l_1 + l_2) - x] \end{aligned} \quad (1)$$

When  $l_2 < x < l_1 + l_2$ ,

$$\begin{aligned} \omega_2 = & \frac{q_1 x^2}{24EI} [x^2 + 6(l_1 + l_2)^2 - 4(l_1 + l_2)x] - \left[ \frac{q_2 l_2^4}{30EI} + l_1 \sin\left(\frac{q_2 l_2^3}{24EI}\right) \right] \\ & - \frac{x^2 F \sin \alpha}{6EI} [3(l_1 + l_2) - x] \end{aligned} \quad (2)$$

Where,  $q_1$  is the uniform load of main roof. From coal wall to load limit equilibrium zone, the load reduce gradually, simplified to a linear change.  $q_2$  is the limit equilibrium load beside the roadway,  $l_1$  is width of roadway main roof,  $l_2$  is the width of integrated coal beside the roadway plastic zone,  $F$  is the force of roof break interface,  $\alpha$  is the roof break angle.

Fig. 2(b) deflection to the roadway side, when  $0 < x < l_2$ ,

$$\begin{aligned} \omega_1 = & \frac{q_1 x^2}{24EI} [x^2 + 6(l_1 + l_2) - 4(l_1 + l_2)x] - \frac{q_2 x^2}{120EI l_2} (10l_2^3 - 10l_2^2 + 5l_2^2 x - x^3) \\ & + \frac{x^2 F \sin \alpha}{6EI} \end{aligned} \quad (3)$$

When  $l_2 < x < l_1 + l_2$ ,

$$\begin{aligned} \omega_2 = & \frac{q_1 x^2}{24EI} [x^2 + 6(l_1 + l_2) - 4(l_1 + l_2)x] - \left( \frac{q_2 l_2^4}{30EI} + l_1 \sin\left(\frac{q_2 l_2^3}{24EI}\right) \right) \\ & + \frac{x^2 F \sin \alpha}{6EI} [3(l_1 + l_2) - x] \end{aligned} \quad (4)$$

$$\omega_1 = \frac{q_1 x^2}{120EI l_2} (10l_2^3 - 10l_2^2 x + 5l_2 x^2 - x^3) - \frac{q_1 x^2}{24EI} (x^2 + 6l_1^2 - 4l_1 x) \quad (5)$$

When  $l_2 < x < l_1 + l_2$ ,

$$\omega_2 = \frac{q_3 l_3^4}{30EI} - \frac{q_1 x^2}{24EI} (x^2 + 6l_1^2 - 4l_1 x) \quad (6)$$

From the analysis above, the different deflection angles of the break roof layer decide the functional expression of the roadway main roof stratum subsidence and will affect the stability of the surrounding rock accordingly. The stress distribution and migration law of overlying rock are important factors affecting the stability of the roadway surrounding rock. As the working face advances, the roadway surrounding rock and overlying rock will be subject to the disturbance of mining at the working face over a long period. The angle of the break roof directly affects the overall caving support effect and pressure release effect of the thick-layer soft rock and is also a key factor affecting the stability of the surrounding rock.

### 3. Establishment of discrete element model

3DEC is a 3D discrete element computational analysis procedure for processing discontinuous medium and used to simulate the response of discontinuous medium, such as joint fissure, etc. in the rock mass under the effect of static load and dynamic load. The Lagrange solution method is used and the mechanical behavior of rock and joint surfaces is processed according to Newton's second law and force-displacement law (Yang *et al.* 2015a and Rebello *et al.* 2014). The elastic nature of the rock mass is obtained through overlaying joint and rock deformation

$$\begin{bmatrix} \varepsilon_{xx} \\ \varepsilon_{yy} \end{bmatrix} = (C^{rock} + C^{jointing}) \begin{bmatrix} \sigma_{xx} \\ \sigma_{yy} \end{bmatrix} \quad (7)$$

Where,  $C^{rock}$  is integrity of isotropic rock,  $C^{jointing}$  is rock joints. Deformation of the matrix

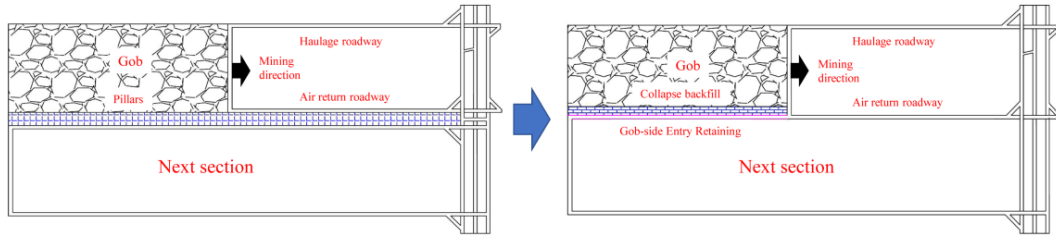
$$C^{rock} = \frac{1+\nu}{E} \begin{bmatrix} 1-\nu & -\nu \\ -\nu & 1-\nu \end{bmatrix} \quad (8)$$

$$C^{jointing} = \begin{bmatrix} \frac{1}{sk_n} & 0 \\ 0 & \frac{1}{sk_n} \end{bmatrix} \quad (9)$$

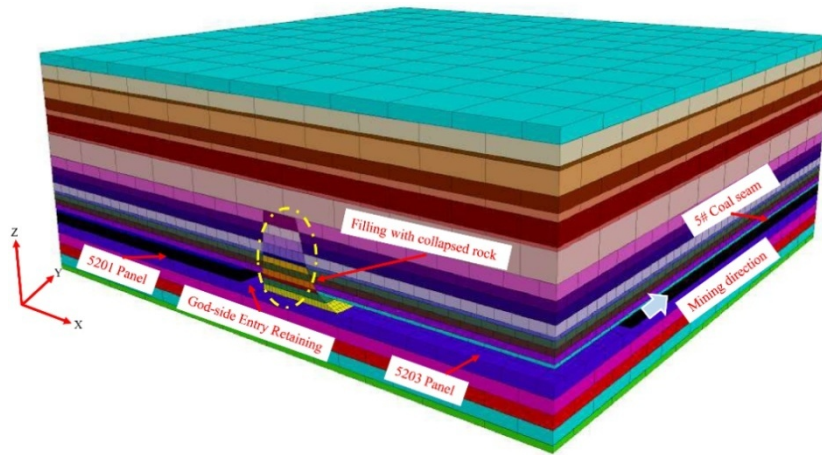
Where,  $s$  is joint spacing,  $k_n$  is joint normal stiffness. Total Poisson ratio effect of joint rock

$$\frac{\sigma_{xx}}{\sigma_{yy}} = \frac{\nu(1+\nu)}{E / (Sk_n) + (1+\nu)(1-\nu)} \quad (10)$$

3DEC discrete numerical model is established herein according to the occurrence characteristic of thick-layer soft rock roof at coal seam 5#. As shown in Fig. 3, its dimensions are 100×105×40, and it includes coal seam 5#, the overlying rock and floor strata. The designed mining thickness of the coal seam is 2 m, the average inclination of the coal seam is 0°, the thickness of the overlying rock at the coal seam is 32 m, and the thickness of the floor stratum is 8 m. The sides of the



(a) Gob-side entry retaining roadway layout



(b) 3DEC discrete numerical model

Fig. 3 Establish a three-dimensional computing model

calculation model are displacement boundaries restricting movement in the horizontal direction and its underside restricts vertical movement. Full-seam mining is applied and the working face advances 5 m in each mining cycle.

After being broken, the rock stratum has a certain breaking coefficient and its volume will cause expansion, so the accumulation height will be greater than the original thickness of the caving overlying rock after caving. The height of rock stratum caving after compaction will depend on the bulking coefficient  $K_p$  of the rock. The rock caving at the roof soft rock caving zone in the working face is irregular. After re-compaction, the loosening coefficient is low and the residual breaking expansion coefficient  $K_p$  is taken as 1.1. When the caving thickness of the overlying rock rock stratum is  $\Sigma h$ , the accumulation height after caving is  $K_p \Sigma h$ . The possible gap remaining with the overlying stable rock stratum is

$$\Delta = \sum h + M - K_p \sum h = M - \sum h(K_p - 1) \tag{11}$$

Where:  $M$  is the mining height, taken as 2 m; is the residual bulking coefficient of rock, taken as 1.2.

According to Eq. (11), when  $M = \Sigma h(K_p - 1)$ ,  $\Delta = 0$ , i.e., the falling overlying rock will fill up the gob to support the load of overlying rock. Thus, the required thickness of the overlying rock to fill up the gob is

Table 1 Physical and mechanical parameters of rock stratum

Parameters	Bulk (GPa)	Shear modulus (GPa)	Tension (MPa)	Cohension (MPa)	Friction (°)	Density (kg.m <sup>-3</sup> )
Sand mudstane	6.5	8.6	2.1	1.2	32	2600
5# Coal seam	1.5	2.0	1.2	0.9	24	2450
Mudstone	4.1	8.6	1.7	1.4	30	2200
Fine sandstone	36	12.6	7.2	1.45	31.5	2600
Silstone	25	4.6	3.6	1.0	33	2500
2# Coal seam	1.5	2.0	1.2	0.9	24	2450

$$\sum h = \frac{M}{K_p - 1} \quad (12)$$

The parameters are entered into Eq. (12) to obtain  $\Sigma h$ , i.e., the required caving height of the break roof layer for the gob-side entry retaining at working face 5203 is 10 m. In the same mesh model, the embedding depth of the coal seam is 200m, the average density of the rock stratum is 2500 kg/m<sup>3</sup>, the initial vertical stress  $p = 5$  MPa is applied at the top of model, and the pressure measuring coefficient is  $\lambda = 1.1$ . During analog computation, the Mohr-Coulomb's failure criterion is employed

$$f_s = \sigma_1 - \sigma_3 \frac{1 + \sin \varphi}{1 - \sin \varphi} + 2C \sqrt{\frac{1 + \sin \varphi}{1 - \sin \varphi}} \quad (13)$$

Where,  $\sigma_1$ ,  $\sigma_3$  are the maximum and minimum main stress, respectively.  $C$ ,  $\varphi$  are the bonding force and frictional angle of the rock. Respectively, when  $f_s > 0$ , the material will experience shear failure. The Mohr-Coulomb's failure criterion can reflect the strength characteristics of rock comprehensively and it is widely applied in underground engineering. When the rock reaches the yield limit, plastic flow will be generated. See Table 1 for the physical and mechanical parameters of rock stratum.

## 4. Analysis of numerical simulation result

### 4.1 Stability analysis for integrated coal beside the roadway of gob-side entry retaining

If the overlying rock of the roadway can form a stable composite beam structure after roof breaking, the deformation of the surrounding rock of the roadway is low; on the contrary, the deformation of the surrounding rock will become stable after a long period and will be increased remarkably (Yang *et al.* 2016). When the integrated coal beside the roadway of gob-side entry retaining is subject to the violent mining influence of the working face, as the distance between the retained roadway section and working face is increased, the high stress generated by movement of overlying thick-layer soft rock stratum will be transferred to the deep part of the integrated coal beside the roadway gradually, causing the deformation migration of deep surrounding rock in a large scope (Yang *et al.* 2015b). The integrated coal beside the roadway will be forced to migrate into the roadway violently. Meanwhile, the shallow surrounding rock of gob-side entry

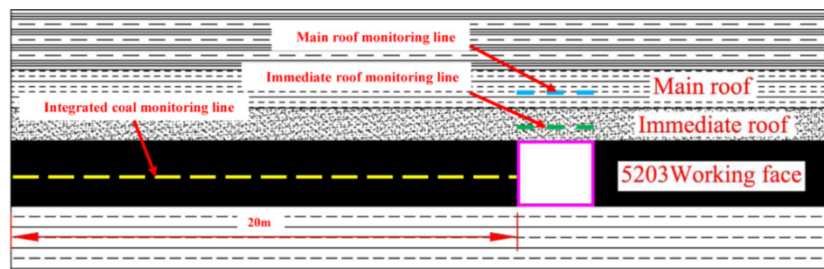


Fig. 4 Monitoring lines layout

retaining is deformed and damaged in a large scope, and the carrying capacity is low. The integrated coal beside the roadway will show shallow fracture development and then become a loose broken body, leading to the inclined subsidence of the roadway roof (Nikadat and Marji 2016). As shown in Fig. 4, monitoring points are set at the side of the integrated coal in the model, roadway roof and at both sides of the roadway. This paper specifies that the break roof layer deflection angle to the roadway side is negative and the deflection to the gob side is positive. At the break roof layer angles of  $-5^\circ$ ,  $0^\circ$ ,  $5^\circ$ ,  $10^\circ$  and  $15^\circ$ , the stress distribution curve within 20 m to the side of the integrated coal beside the roadway at gob-side entry retaining at 10 m, 30 m, 50 m and 70 m behind the working face of gob-side entry retaining mining system is shown in Fig. 5.

Figs. 5(a), (b) and (e) show the stress curves at the side of the integrated coal beside the roadway of gob-side entry retaining at the break roof layer angles of  $-5^\circ$ ,  $5^\circ$ ,  $10^\circ$ . At 10 m behind the working face, the roadway roof is at the initial hanging state. The supporting peak stress is located at 4.5-5 m from the roadway edge, the peak stress is 8.5-9 Mpa and the stress concentration factor is 1.48-1.57. At 30 m behind the working face, the surrounding rock of the integrated coal body has good integrity. The peak stress of the integrated coal beside the roadway is transferred to the deep part, and its bearing capacity is increased rapidly. The supporting peak stress is located at 6.25-7.25 m from the roadway edge, the peak stress is 9.65-10.1 Mpa and the stress concentration factor is 1.68-1.75. At 50 m behind the working face, the stress of the integrated coal body is increases rapidly. The integrated coal body serves as the supporting point of the main roof, and its vertical stress will be increased continuously. The maximum vertical stress at the side of the integrated coal body will be increased to 11.1-12.8 Mpa and the stress concentration factor reaches 1.93-2.22. At 70 m behind the working face, the main roof is gradually supported by gangue from the gob, so the roof activity tends to be stable. The surrounding rock stress will be transferred further to the deep part. The vertical stress of the integrated coal body is reduced to some extent. Accordingly, the integrated coal body, filling body and gangue from the gob jointly maintain the stability of the roof.

At the roof breaking inclination angle of  $0^\circ$  and  $15^\circ$ , the stress level at the side of the integrated coal is high, and the peak stress is further transferred to the deep part of coal body, as shown in Figs. 5(b) and (d). At 10 m behind the working face, the supporting peak stress is located at 5-6.25 m from the roadway edge, the peak stress is 9.5-10.05 Mpa and the stress concentration factor is 1.65-1.75. At 30 m behind the working face, the supporting peak stress is located at 6.5-7.5 m from the roadway edge, the peak stress is 10.05-11 Mpa and the stress concentration factor is 2.17-2.35. At 70 m behind the working face, the peak stress is transferred to the deep part of the coal body continuously, and is located at 7.5-8.75 m from the roadway edge. The peak integrated coal body stress is 12.5-14 Mpa and the stress concentration factor is 2.17-2.43.

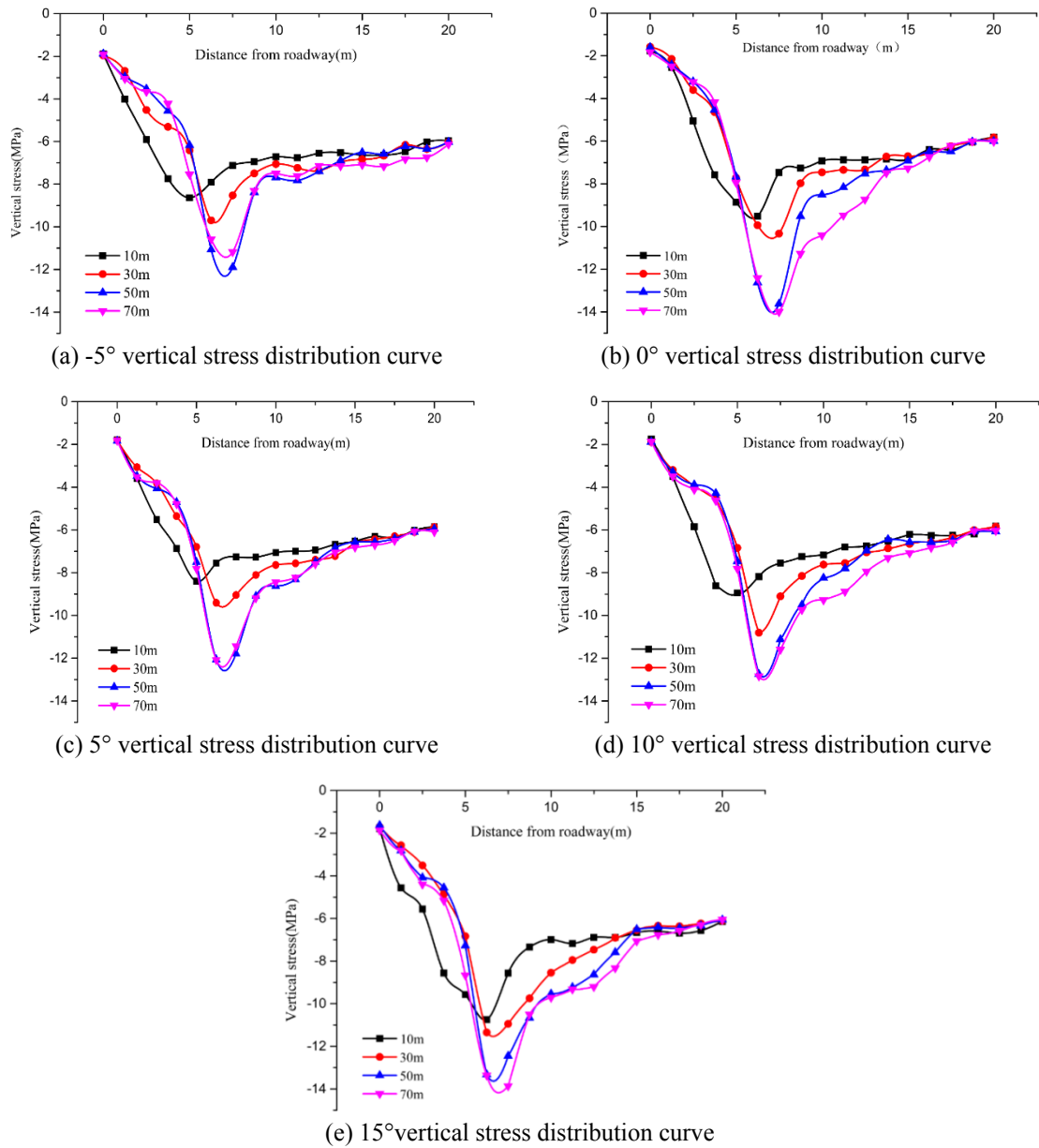


Fig. 5 Integrated coal beside the roadway vertical stress distribution curve

At 50 m behind the working face, the pressure of the integrated coal beside the roadway appears to be the most violent. The sink rate of its roof is the highest, and is mainly reflected as tension fracture damage and shear slip damage. Its shaping scope is shown in Fig. 6. At the break roof layer angles of  $-5^\circ$ ,  $5^\circ$ ,  $10^\circ$ , the pressure-releasing loose area is 0-1.25 m from the roadway surface. Subject to the supporting pressure, the coal body will suffer deformation and yield damage, and its supporting capacity will be reduced significantly; the shaping bearing zone is 1.25-4.5 m from the roadway surface. The coal body destruction is weak and the supporting

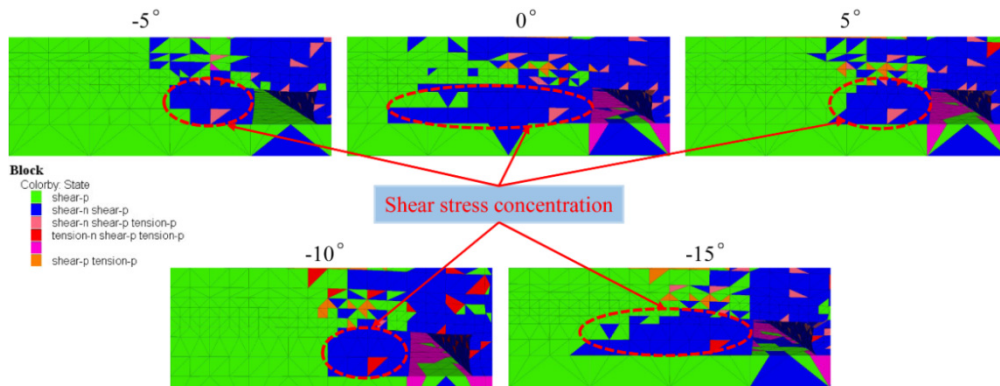


Fig. 6 Integrated coal beside the roadway plastic zone distribution

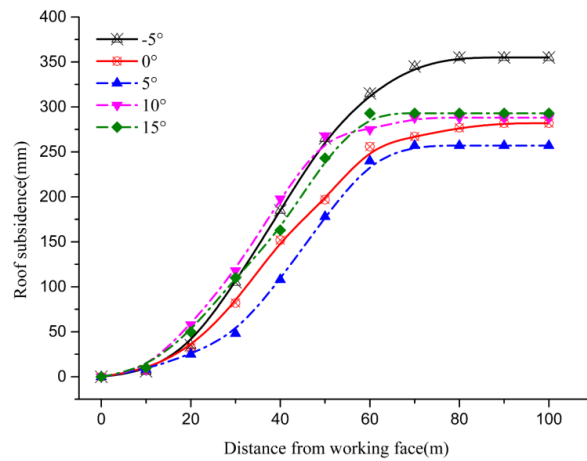


Fig. 7 Integrated coal beside the roadway roof subsidence curve

pressure is transferred to the deep part of the coal body. The elastic deformation area is 4.5-8.75 m from the roadway surface. The coal body has good stability and can bear high stress and maintain an elastic state. At the break roof layer angles of 0° and 15°, the supporting stress at the side of the integrated coal beside the roadway and stress concentration factor are high, so the plastic damage is severe, and the pressure-releasing loose area is expanded, 0-2.5 m from the roadway surface. The shaping bearing zone is 2.5-5 m from the roadway surface and the elastic deformation zone is 5-8.75 m from the roadway surface.

Fig. 7 is the subsidence curve of the roof at the side of the integrated coal. At 10-60 m behind the working face, the displacement tends to present linear change. At the roof breaking inclination angles of -5°, 10° and 15°, the slope of the curve is great. During the extraction at the working face, the roof deformation at the side of the integrated coal beside the roadway is acute; at more than 60 m behind the working face, the roof settling tends to be stable. At roof breaking inclination angles of -5°, 0° and 5°, the roof subsidence is below 300 mm. At break roof layer angles of 10° and 15°, the roof subsidence is above 350 mm with the increase rate of 16%. Thus, the roof settling is evident.

### 4.2 Stability analysis of roadway roof

The integrated coal body is located at one side of the gob-side entry retaining, and the filling body is located at the other side. The roof deformation is asymmetric. At the rear of the working face, the roof rotates and sinks toward the gob. The large-scale shear failure is caused on the roof above the gob (Bai *et al.* 2015 and Ma *et al.* 2016). As the fracture of overlying rock at the side of gob sinks, the disturbance on the roadway roof will be increased, the scope of shear slip and tearing crack growth will be enlarged, and the abscission layer between layers at the same position will be widened, which will significantly reduce the carrying capacity of the rock stratum, thus, the stability of surrounding rock is seriously threatened (Li *et al.* 2016b). Fig. 9 shows the midpoint vertical displacement and stress curve of the immediate roof and main roof of the roadway behind the working face at the roof breaking inclination angles of  $-5^\circ$ ,  $0^\circ$ ,  $5^\circ$ ,  $10^\circ$  and  $15^\circ$ , respectively. The red-dot distribution area indicates a tensile damage state between rock strata.

At 20 m behind the working face, the overlying strata at the side of gob collapse along the roof breaking line, and bend and sink when the gob side of the roadway is at the initial hanging state. The vertical stress is reduced dramatically. Meanwhile, the caving filling body gradually makes contact with the roof at the side of the roadway gob and supports it. Then, the vertical stress will be increased. The subsidence of the immediate roof and main roof shows little difference, forming the characteristic coordinated movement.

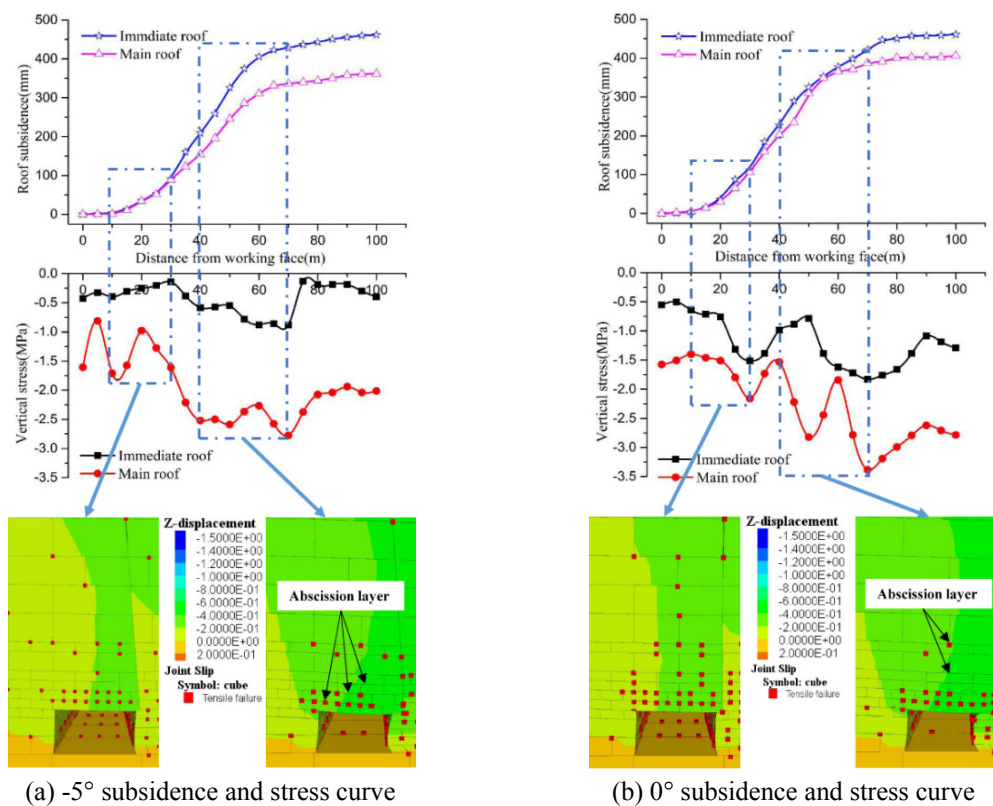
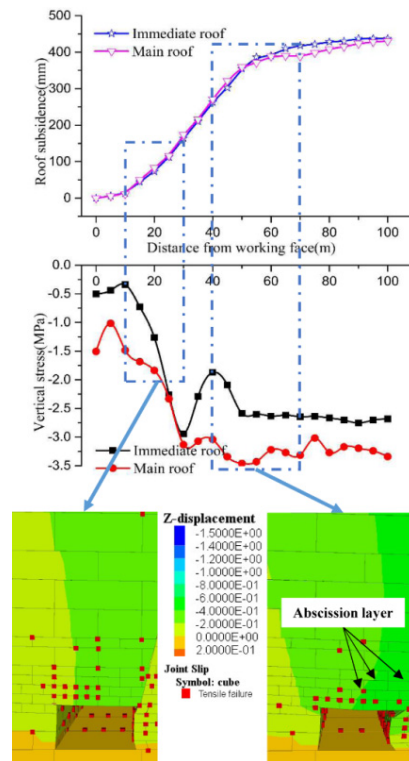


Fig. 8 Roof subsidence and stress curve





(e) 15°subsidence and stress curve

Fig. 8 Continued

strata. At 40 m behind the working face, the roof sinks quickly with great subsidence. At 80 m behind the working face, the roof sinks with a gradual reduction of speed. At more than 80 m behind the working face, the roof settling tends to be stable. At the break roof layer angles of 10° and 15°, the hanging area of the roadway roof is large. At 20-40 m behind the working face, the vertical displacement of rock strata on the immediate roof and main roof significantly increases. The slope of the subsidence curve is increased, and the roadway roof sinks acutely, causing an intense dynamic load effect; as shown in Fig. 8(c), at 20 m behind the working face, the pressure of the immediate roof and main roof is stable, weakening the dynamic pressure effect of overlying rock during the subsidence. Meanwhile, the vertical displacement curve tends to coincide, forming coordinated movement, so the abscission layer is not liable to appear.

#### 4.3 Stability analysis of roadway at the filling side

The roof contact of the break roof layer caving and overlying stable rock greatly restricts the activity space of the roadway roof, eliminates the hanging roof, reduces the overlying cantilever load and rotational deformation force, effectively reduces the disturbance roof activity has on the surrounding rock of the roadway and optimizes the stress environment of the roadway (Zhang *et al.* 2012 and Małkowski 2015). As the working face advances, the roof will be bent, broken and sink rotationally at the side of the roadway gob (Li *et al.* 2016c and Yong *et al.* 2015). The rotational deformation will occur on the thick-layer soft overlying strata structure along the roof

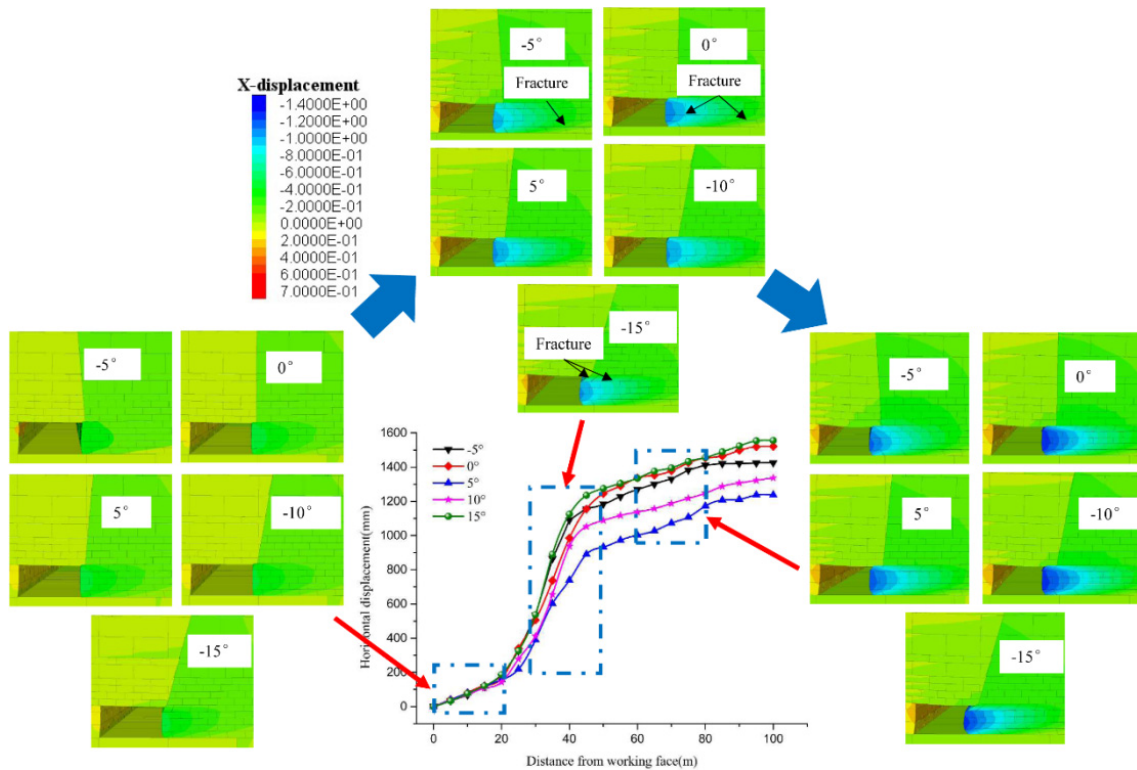


Fig. 9 The side of roof break and filling horizontal displacement curve nephogram

breaking interface above the entry retaining to the gob side. The stress on the roof above the filling body close to the gob side will be increased continuously. The filling body is not only subject to the vertical pressure, but also to the increasing horizontal thrust (Chen *et al.* 2016 and Yoo 2016). Frictional resistance will be generated between the caving filling body and the coal seam floor. When the horizontal thrust is larger than the frictional resistance, the caving filling body will lose stability, endangering the stability of the surrounding rock of the roadway.

As shown in Fig. 9, at 20 m behind the working face, the roadway roof does not reach the limit breaking distance. The caving filling body does not play a supporting role and no evident lateral displacement occurs at the side of the roadway gob. At 20-50 m behind the working face, the lower rock stratum at is fragmented, and the rotational subsidence is great for a short period. An acute disturbance is caused to the lateral caving filling rock. At the break roof layer angles of 0°, 10° and 15°, the roof has an evident inclined downward thrust effect on the caving filling body. Meanwhile, multiple longitudinal and crosswise splitting failures appear, and the displacement of filling body gangue into the roadway is increased rapidly. The caving gangue is liable to swarm into the roadway. At the break roof layer angles of -5° and 5°, the connection of roadway and roof strata at the gob side is cut to weaken the horizontal displacement; at 50-85 m behind the working face, the higher rock stratum will break the subsidence, mainly to apply pressure to the caving filling body through slow sinking. Subject to the compression of overlying strata, the deformation will continue. At this moment, the slope of the lateral horizontal displacement curve is reduced; at more than 85-90 m behind the working face, the influence of mining ends and the horizontal

displacement ends. At the break roof layer angles of  $0^\circ$ ,  $10^\circ$  and  $15^\circ$ , the horizontal displacement after stabilization is evidently larger than that at the break roof layer angles of  $-5^\circ$  and  $5^\circ$ .

At 50 m behind the working face, the shaping distribution of the caving filling body at the side of the roadway gob is shown in Fig. 10. At the break roof layer angles of  $-5^\circ$ ,  $10^\circ$  and  $15^\circ$ , partial shear stress concentration appears at the end of the roadway break roof layer and moves toward the center position above the filling body. At the break roof layer angle of  $0^\circ$ , shear stress concentration distributed along the break roof layer interface will be generated. At the break roof layer angle of  $5^\circ$ , the shear stress concentration of the caving filling body is weakened. When there is a great load on the filling body, the roof and floor close to the rock stratum also assume a corresponding load. When the stress concentration scope is large, the lateral slip is liable to occur on the filling body and its load-carrying properties can't be fully utilized.

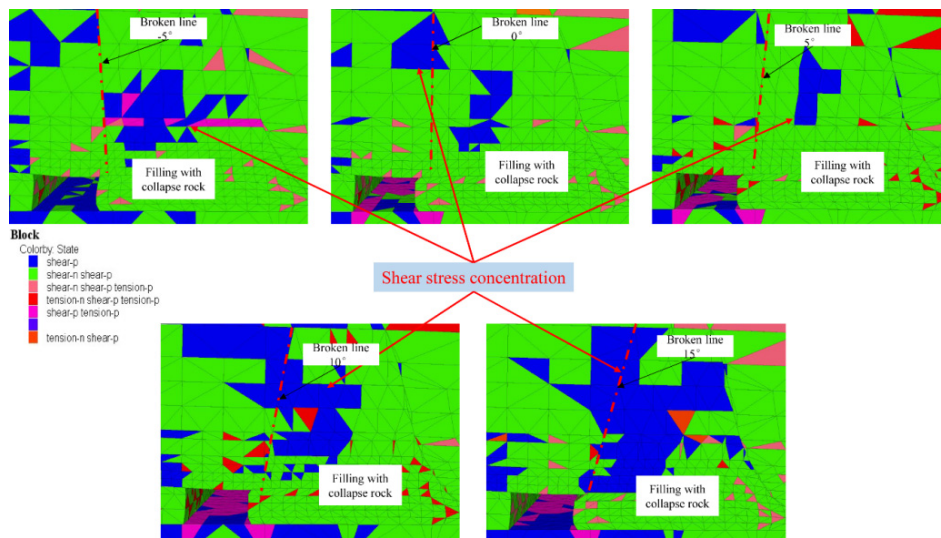


Fig. 10 The side of roof break and filling plastic zone distribution

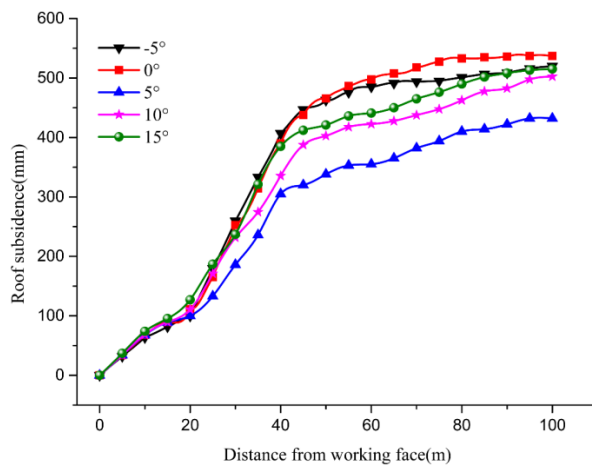
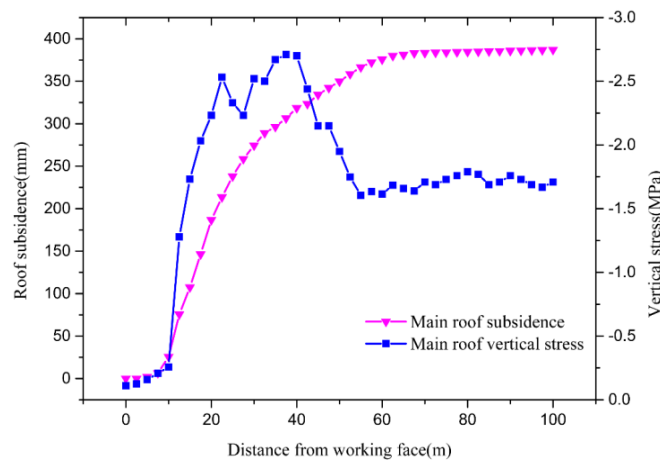
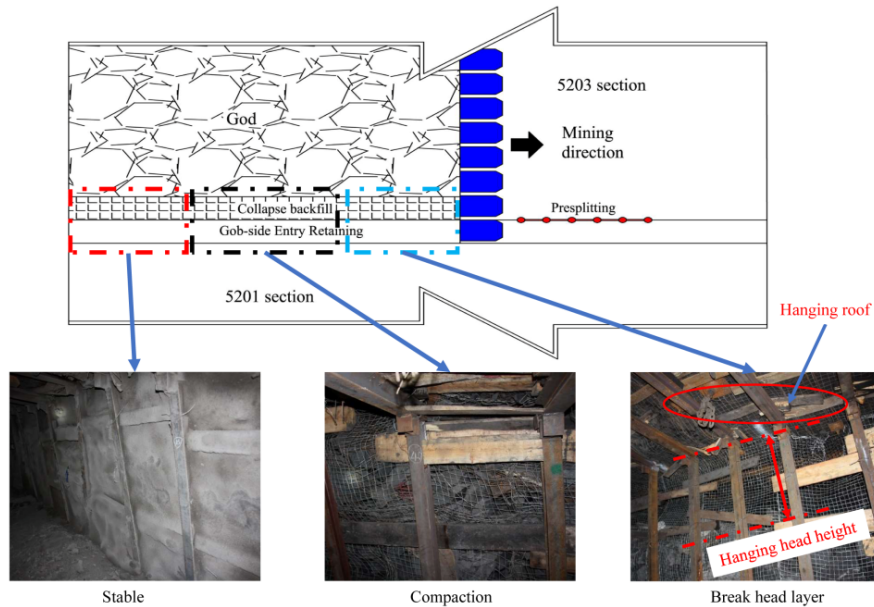


Fig. 11 The side of gob roof subsidence and stress curve

The subsidence curve of the roof at the side of roadway gob is shown in Fig. 11. At 0-50 m behind the working face, the slope of the subsidence curve is large. The subsidence of the roof at the break roof layer angles of  $-5^\circ$ ,  $0^\circ$  and  $15^\circ$  is the most severe. During the rotation of the breaking roof, squeezing action is generated to the side of roadway gob to some extent. The caving filling body at the roof break layer angle can't effectively support the roof strata at the side of roadway gob. The displacement slip occurs on the roadway roof and the immediate roof is separated and damaged. The vertical displacement is acute. At the break roof layer angle of  $5^\circ$ , the intensity of roof subsidence is mitigated, effectively maintaining the stability of the surrounding rock of gob-side entry retaining.



(a) Field monitoring data



(b) The field test in 5203 roadway

Fig. 12 Field test and monitoring data

## 5. Field test

At the air-return roadway at the section of 5203 working face Changxing coal mine, deflection of  $5^\circ$  to the side of the roadway gob is used as the break roof layer inclination angle to implement the filling of gob-side entry retaining on the break roof layer with the height of 10 m. Meanwhile, the displacement and pressure monitoring stations are allocated every 2.5 m at the side of roadway gob.

As shown in Fig. 12, the caving filling section is located at 0-35 m behind the working face. The connection of the roadway and overlying rock of the gob is cut to form large-area hanging roof without fracturing. The weight of the lateral residual main roof is fully assumed by the integrated coal body of the roadway. The lower rock strata at the rear of the working face have weak resistance to disturbance. After small-area exposure, the overlying rock at the side of the gob collapses in layers from bottom to top. The roadway roof is not broken and doesn't sink. The roof at the side of the gob comes into contact with the caving filling body and is squeezed and fixed into the entry under the pressure effect of the overlying rock. This section is located at the pressure reduction zone behind the working face, and the subsidence of the roadway roof is 200-250 mm. The compaction section is located 35-75 m behind the working face. The pressure of overlying strata at the side of the gob on the filling body of the break roof layer is increases as the distance from the coal wall of the working face increases. After collapse, the soft rock strata are broken, and the skeleton structure formed is small, further accelerating the closing of the gaps between rocks. The caving filling body is continuously compacted and the carrying capacity is gradually recovers, coming close to the stress of primary rock. The vertical displacement of the roof at this stage is 80-100 mm. The section with a tendency to stability is located at 75-100 m behind the working face. As the stress is increased, the caving filling rock starts breaking in a greater amount, and irreversible compression deformation is caused. The broken granules are filled into the hole. The porosity in the gravel is reduced, the deformation resistance of the gravel structure is gradually enhanced and the subsidence of the roadway roof is sharply decelerated (Komurlu and Kesimal 2015). The vertical displacement of the roof at this section is 30-50 mm. The filling body of the break roof layer gradually reaches a supporting force which tends stabilizes in the end.

As shown in Fig. 13, the deformation law of the main roof rock stratum located on the

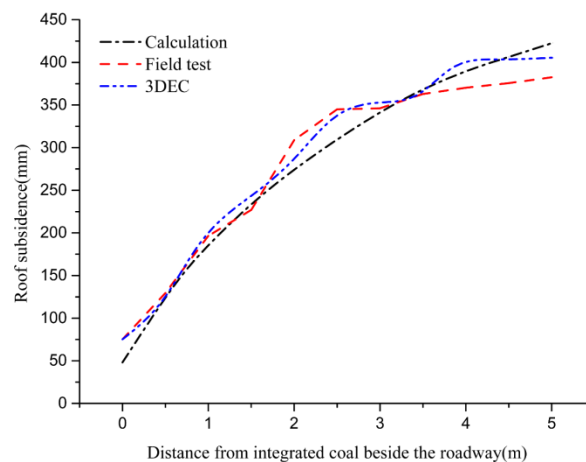


Fig. 13 Main roof subsidence curve

immediate roof has a direct impact on the stability of the roadway. The monitoring points for the main roof in the numerical simulation model and the deep hole displacement meters for the roadway roof on site are monitored. Relevant parameters are brought into Eqs. (1)-(2) to plot the subsidence curve of the roadway main roof from the integrated coal side to the roadway gob side. As shown in Eq. (13), the variation tendency is basically consistent. At the range of 0-1m at the side of the integrated coal beside the roadway, the subsidence of the main roof is mainly due to the plastic deformation of shallow integrated coal, and the subsidence is small; at 1-3.5 m, the curve slope of the main roof rock stratum has a great change under the combined effect of rotational subsidence and bending deformation, and the subsidence speed is increased; the caving filling body of 3.5-5 m plays a supporting role for the main roof, and its curve tends to be stable.

## **6. Conclusions**

- (1) With respect to the occurrence characteristics of thick-layer soft rock roof coal seam strata, such as low strength, fracture development, weak carrying capacity and no key pressure-bearing layer, etc., the new technology of filling gob-side entry retaining on the break roof layer is proposed with the core of “roof breaking and pressure releasing + filling caving with rock”. Meanwhile, the vertical displacement distribution function of the main roof for gob-side entry retaining is obtained for different directions of the break roof layer on the basis of different boundary conditions of the roadway main roof as per the direction of the break roof layer.
- (2) The 3D discrete element calculation model is established at the break roof layer angles of  $-5^\circ$ ,  $0^\circ$ ,  $5^\circ$ ,  $10^\circ$  and  $15^\circ$  to analyze the vertical stress distribution features and plastic damage scope at the side of the integrated coal beside the roadway. At the break roof layer angles of  $0^\circ$  and  $15^\circ$ , the roadway lateral supporting stress acutely changes, the scope of plastic damage is large and the subsidence of the roadway roof at the side of the integrated coal is greatly subsides. At the break roof layer angles of  $-5^\circ$  and  $0^\circ$ , the changes of vertical displacement and vertical stress of the immediate roof and main roof are not coordinated, and shear stress concentration is formed partially. Slip failure occurs between rock strata, which are liable to cause large-scale separation of roadway overlying rock. At the break roof layer angles of  $10^\circ$  and  $15^\circ$ , the large-area shear stress concentration is generated on the interface of the break roof layer, and the subsidence of the roadway gob acutely subsides. At the break roof layer angles of  $5^\circ$ , the stress concentration at the side of the integrated coal beside the roadway is reduced to mitigate the disturbance to the roadway roof and loss of carrying capacity caused by mining. The caving filling body effectively supports the overlying rock at the side of the roadway gob. Accordingly, the stress environment of the gob-side entry retaining area is optimized.
- (3) The filling of quick gob-side entry retaining on the thick-layer soft roof break roof has been implemented at the air return roadway of working face 5203 at the mine in Changxing, Shanxi Province, China by application of the gob-side entry retaining scheme at the break roof layer angle of  $5^\circ$ . The difficulty of gob-side entry retaining at the thick-layer soft rock stratum has been solved effectively and a good application effect has been achieved. Meanwhile, the monitoring data from the roof pressure and displacement monitoring points allocated on site indicates that the caving filling section is located at 0-35 m behind the working face, the compaction section is located at 35-75 m and the stable section is located at 75-100 m.

## Acknowledgments

This study is supported by National Natural Science Foundation of China (Nos. 51323004, 51674250 and 51074163), the Trans-Century Training Programme Foundation for the Talents by the State Education Commission (No. NCET-08-0837), the State Key Program of National Natural Science of China (No. 50834005), the Fundamental Research Funds for the Central Universities (Nos. 2010QNB25 and 2012LWB66), the Natural Science Foundation of Jiangsu Province (No. BK2009092), the “Six major talent” plan of Jiangsu Province, the Graduate Innovative Foundation of Jiangsu Province (NO. CXZZ13\_0924), Open Fund of State Key Laboratory for Geomechanics and Deep Underground Engineering (No. SKLGDUEK1409).

## References

- Bai, J.B., Shen, W.L., Guo, G.L., Wang, X.Y. and Yu, Y. (2015), “Roof deformation, failure characteristics, and preventive techniques of gob-side entry driving heading adjacent to the advancing working face”, *Rock Mech. Rock Eng.*, **48**(6), 2447-2458.
- Chen, M., Yang, S.Q., Zhang, Y.C. and Zang, C.W. (2016), “Analysis of the failure mechanism and support technology for the Dongtan deep coal roadway”, *Geomech. Eng., Int. J.*, **11**(3), 401-420.
- Fan, K., Liu, G., Xiao, T. and Zheng, L. (2010), “Study on overlying strata movement and structure features aroused by mountainous shallow buried coal seam mining”, *Proceedings of International Conference on Mine Hazards Prevention and Control*, Qingdao, China, October, pp. 76-82.
- Komurlu, E. and Kesimal, A. (2015), “Sulfide-rich mine tailings usage for short-term support purposes: An experimental study on paste backfill barricades”, *Geomech. Eng., Int. J.*, **9**(2), 195-205.
- Li, X. and Li, W. (2016), “Numerical investigation on fracturing behaviors of deep-buried opening under dynamic disturbance”, *Tunn. Undergr. Sp. Tech.*, **54**, 61-72.
- Li, H., Zhao, B., Guo, G., Zha, J. and Bi, J. (2016a), “The influence of an abandoned goaf on surface subsidence in an adjacent working coal face: A prediction method”, *Bull. Eng. Geol. Environ.*, 1-11.
- Li, S.C., Wang, J.H., Chen, W.Z., Li, L.P., Zhang, Q.Q. and He, P. (2016b), “Study on mechanism of macro failure and micro fracture of local nearly horizontal stratum in super-large section and deep buried tunnel”, *Geomech. Eng., Int. J.*, **11**(2), 253-267.
- Li, X., Ju, M., Yao, Q., Zhou, J. and Chong, Z. (2016c), “Numerical investigation of the effect of the location of critical rock block fracture on crack evolution in a gob-side filling wall”, *Rock Mech. Rock Eng.*, **49**(3), 1041-1058.
- Ma, T., Wang, L., Suorineni, F.T. and Tang, C. (2016), “Numerical analysis on failure modes and mechanisms of mine pillars under shear loading”, *Shock Vib.*, **2016**(1), 1-14.
- Małkowski, P. (2015), “The impact of the physical model selection and rock mass stratification on the results of numerical calculations of the state of rock mass deformation around the roadways”, *Tunn. Undergr. Sp. Tech.*, **50**, 365-375.
- Nguyen, T.L., Hall, S.A., Vacher, P. and Viggiani, G. (2011), “Fracture mechanisms in soft rock: identification and quantification of evolving displacement discontinuities by extended digital image correlation”, *Tectonophysics*, **503**(1-2), 117-128.
- Nikadat, N. and Marji, M.F. (2016), “Analysis of stress distribution around tunnels by hybridized FSM and DDM considering the influences of joints parameters”, *Geomech. Eng., Int. J.*, **11**(2), 269-288.
- Ning, J., Wang, J., Liu, X., Qian, K. and Sun, B. (2014), “Soft–strong supporting mechanism of gob-side entry retaining in deep coal seams threatened by rockburst”, *Int. J. Min. Sci. Tech.*, **24**(6), 805-810.
- Rebello, N., Sastry, V.R. and Shivashankar, R. (2014), “Study of surface displacements on tunnelling under buildings using 3dec numerical modelling”, *International Scholarly Research Notices*.
- Taheri, A. and Tani, K. (2010), “Characterization of a sedimentary soft rock by a small in-situ triaxial test”, *Geotech. Geol. Eng.*, **28**(3), 241-249.

- Tan, Y.L., Yu, F.H., Ning, J.G. and Zhao, T.B. (2015), "Design and construction of entry retaining wall along a gob side under hard roof stratum", *Int. J. Rock Mech. Min. Sci.*, **77**, 115-121.
- Wang, G.F., Gong, S.Y., Dou, L., Cai, W. and Mao, Y. (2015), "Evolution of stress concentration and energy release before rock bursts: Two case studies from Xing'an Coal Mine, Hegang, China", *Rock Mech. Rock Eng.*, 1-9.
- Yang, J.X., Liu, C.Y., Yu, B. and Wu, F.F. (2015a), "The effect of a multi-gob, pier-type roof structure on coal pillar load-bearing capacity and stress distribution", *Bull. Eng. Geol. Environ.*, **74**(4), 1-7.
- Yang, Y., Wang, R., Xing, W. and Cheng, L. (2015b), "Analysis of deformation and failure of hard rock mass surrounding underground openings in houziyan hydropower station by 3dec numerical simulation", *Apmis Supplementum*, **117**(127), 55-59.
- Yang, X.L., Xu, J.S., Li, Y.X. and Yan, R.M. (2016), "Collapse mechanism of tunnel roof considering joined influences of nonlinearity and non-associated flow rule", *Geomech. Eng., Int. J.*, **10**(1), 21-35.
- Yong, Y., Tu, S., Zhang, X. and Bo, L. (2015), "Dynamic effect and control of key strata break of immediate roof in fully mechanized mining with large mining height", *Shock Vib.*, **2015**(4), 1-11.
- Yoo, C. (2016), "Effect of spatial characteristics of a weak zone on tunnel deformation behavior", *Geomech. Eng., Int. J.*, **11**(1), 41-58.
- Zhao, C. (2015), "Analytical solutions for crack initiation on floor-strata interface during mining", *Geomech. Eng., Int. J.*, **8**(2), 237-255.
- Zhu, H., Ye, B., Cai, Y. and Zhang, F. (2013), "An elasto-viscoplastic model for soft rock around tunnels considering overconsolidation and structure effects", *Comput. Geotech.*, **50**(50), 6-16.
- Zhang, G.F., He, M.C., Yu, X.P. and Huang, Z.G. (2011), "Research on the technique of no-pillar mining with gob-side entry formed by advanced roof caving in the protective seam in Baijiao coal mine", *J. Min. Saf. Eng.*, **28**(4), 511-516. [In Chinese]
- Zhang, N., Yuan, L., Han, C., Xue, J. and Kan, J. (2012), "Stability and deformation of surrounding rock in pillarless gob-side entry retaining", *Safety Sci.*, **50**(4), 593-599.